Journal of Chemical Health Risks

www.jchr.org

ORIGINAL ARTICLE

Antimicrobial Potentials of Iron Oxide and Silver Nanoparticles Green-Synthesized in *Fusarium solani*

Masoomeh Sasani[1], Ebrahim Fataei[*1], Reza Safari[1,2], Fatemeh Nasehi[1], Marzieh Mosayebi[1]

[1]*Department of Environment, Ardabil Branch, Islamic Azad University, Ardabil, Iran*

[2]*Caspian Sea Ecology Research Center, Iranian Fisheries Research Institute, Agricultural Research, Education and Extension Organization , Sari, Iran*

(Received: 17 April 2021 Accepted: 5 July 2021)

KEYWORDS

Green Synthesis;
Silver Nanoparticles;
Iron Oxide Nanoparticles;
Fusarium solani;
Antibacterial Properties

ABSTRACT: The current study aimed to synthesize, characterize and determine the antibacterial activity of iron oxide (Fe_3O_4 NPs) and silver nanoparticles (AgNPs) green-synthesized using *Fusarium solani*. Fungal mass was applied to produce NPs, followed by analyzing NPs using scanning electron microscopy, X-ray diffraction, and Fourier transform infrared spectroscopy. The antimicrobial test was performed by the agar well diffusion method and the microdilution protocol (determining the minimum inhibitory concentration or MIC and the minimum bactericidal concentration or MBC) against *Staphylococcus aureus*, *Bacillus cereus*, *Pseudomonas aeruginosa* and *Escherichia coli*. The highest optical densities for produced AgNPs and Fe_3O_4 NPs were detected at 420 and 215 nm, with a spherical shape and size of 27.5-58.3 nm and a cubic-spherical shape and size of 55.3-84.2 nm, respectively. Ag NPs had more antibacterial activity than Fe_3O_4 NPs, but they were not significantly different in most cases. The most sensitive and resistant bacteria were *S. aureus* and *P. aeruginosa* for both NPs, with the MIC of 10 and 40 µg ml^{-1} as well as the MBC of 20 and 80 µg ml^{-1} for Ag NPs against *S. aureus* and *P. aeruginosa*, respectively. The results were weaker for Fe_3O_4 NPs than for Ag NPs, with the MIC of 20 µg ml^{-1} for *B. cereus* and *S. aureus*, and 40 µg ml^{-1} for *P. aeruginosa* and *E. coli*, with the MBC of 40 and 80 µg ml^{-1}, respectively. The antibacterial properties of the produced NPs indicated that these antimicrobial agents were highly reactive and prevented the growth of unwanted microorganisms.

INTRODUCTION

Nanostructures have recently been considered in various advanced industries, such as medicine, water and wastewater treatment, antimicrobials, diagnostic techniques, pharmaceuticals and food industry, owing to their unique properties, including special optical, electrical, chemical, magnetic, and mechanical features [1].

Silver (Ag) is widely used in traditional medicine, modern medical sciences and pharmaceutical industries owing to its antimicrobial and antiseptic potential. Numerous Ag properties are improved, including contact surface and dispersion during the production of silver nanoparticles (AgNP), particularly using green synthesis methods, thereby increasing the antimicrobial activity of the synthesized fine particles compared to conventional silver [2]. Small-sized NPs can be easily directed into pathogenic and harmful bacterial cells; this influences intracellular processes, such as synthesis of DNA, RNA and proteins, and subsequently inhibits microbial growth [3]. In addition to AgNPs, iron oxide (Fe_3O_4) NPs are produced due to alterations in electromagnetic properties [4].

The fabrication of NPs exploiting green methods using fungi, bacteria and plants has recently received

*Corresponding author: ebfataei@gmail.com (E. Fataei)
DOI: 10.22034/jchr.2021.1928198.1293

considerable attention owing to their unique properties, such as simplicity, low-cost, controllability, non-toxicity, high efficiency and biocompatibility [4, 5 and 6]. In such methods, microorganisms exposed to metal ion salts regenerate these nano-materials via catalytic mechanisms extracellularly or intracellularly [4, 7]. According to the antibacterial properties of produced NPs, higher potential has been reported for extracellular NPs in impeding pathogenic bacterial growth as compared to intracellular NPs [7, 8]. Recently, AgNPs have been biosynthesized using *Fusarium oxysporum* to evaluate antibacterial and anticancer properties. They reported that the nanoparticles produced had a round shape with a size of 5-13 nm. The produced NPs exhibited inhibitory effects against *E. coli* and Staphylococcus with a minimum inhibitory concentration (MIC) of 80 µg $cm^{-3}$and a minimum bactericidal concentration (MBC) of 23.12 µg cm^{-3} [9]. AgNPs in *F. oxysporum* were also synthesized to determine antimicrobial potential. The filtered fungal supernatant contained AgNPs with the highest optical density (OD) at 440 nm. The results also indicated that the produced AgNPs had antimicrobial effects on *Candida albicans*, *E. coli*, *Candida krusei*, *S. aureus* and *Aspergillus flavus* [10].

The present study evaluated the green synthesis of AgNPs and Fe_3O_4 NPs using *Fusarium oxysporum* to determine their qualitative and antibacterial properties. In terms of novelty, our eco-friendly metal nanoparticles can serve as promising bio-alternatives to reduce or eliminate microbial contaminants, especially bacteria, and to avoid additional consumption of environmentally harmful chemicals, particularly chlorine. The high reactivity of metal NPs, even in much lower amounts, can reduce the microbial load of indicator bacteria in water.

MATERIALS AND METHODS

Preparation of iron oxide and silver nanoparticles

In our study, lyophilized *Fusarium solani* obtained from the microbial collection of the Iranian Research Organization for Science and Technology (IROST) was frozen at -18°C. The fungal mass was applied to produce NPs, thus 2 g of biomass was added to 100 ml of a 2-mM silver nitrate solution and mixed in a dark place at 28°C and 150 rpm for 72 h (pH=7). Next, the solution color changed from yellow to dark brown, demonstrating the initial confirmation of AgNPs. A control sample was considered to be a 2-mM silver nitrate solution without fungal mass; the color of the control sample remained yellow and unchanged at the end of the storage period. To fabricate Fe_3O_4 NPs, 2 g of the fungal biomass was added to 50 ml of a 2-mM iron oxide (Fe_2O_3) solution, followed by adjusting pH to 7.5. The samples were incubated in a dark condition at 28°C and 150 rpm for 5 days. The solution color changed from brick red to black, indicating the initial confirmation of Fe_3O_4 NPs; the control sample was considered to be a 2-mM iron oxide solution without fungal biomass [4, 11]. The produced AgNPs and Fe_3O_4 were separated by centrifugation at 6000 rpm for 6 min and at 7000 rpm for 15 min, respectively. The resulting supernatant was collected (to evaluate the extracellular production of nanoparticles) and filtered using a 0.22-micron filter, followed by drying at 45°C [11].

Spectrophotometry was used to confirm the NP production. For this purpose, the OD values of the samples were read before the suspension containing NPs in the range of 300-500 nm and 200-300 nm for AgNPs and Fe_3O_4 NPs, respectively. Initially, 200 µl of NPs were separately diluted into 1 L of distilled water to read their OD at an ambient temperature. Untreated silver nitrate and iron oxide suspensions in distilled water were also utilized as blanks [4, 12].

A scanning electron microscope (SEM) determined the morphological characteristics of the generated NPs. First, a determined volume of NPs was centrifuged at 10,000 rpm for 10 min. After discarding the supernatant, the resulting precipitate was added with distilled water and re-centrifuged in triplicate. A certain amount of ethanol 96% was poured onto the final precipitate, and centrifugation was repeated similar to the previous steps. The supernatant was discarded, and the precipitate was dried at 40°C for two days and prepared for SEM imaging. Then, the average size of nanoparticles was measured by calculation, and its shape was recorded [4, 12].

Characterization of antibacterial potentials

AgNPs and Fe_3O_4 NPs were evaluated for antibacterial activity on the standard bacteria of Staphylococcus *aureus* (PTCC 1112), *Bacillus cereus* (PTCC 1015), *Pseudomonas aeruginosa* (PTCC 1074) and *Escherichia coli* (O157H7) from the IROST.

The agar well diffusion method was performed to measure the antibacterial activities. Thus, 20 µl of the studied bacterial suspension (with 1.5×10^8 CFU ml^{-1} equivalent to 0.5 McFarland standard turbidity) was cultured onto the Mueller Hinton agar (MHA) medium. The calculated inhibitory zone diameter (ZOI) concentrations were 50 and 100 µg $cm^{-3}$of AgNPs and Fe_3O_4 NPs, which were sonicated at 40 kHz for half an hour to prepare a homogeneous suspension and poured into 7-mm wells embedded in the medium. The ampicillin (as a gram-positive bacterium) and gentamicin (as a gram-negative bacterium) were regarded as a positive control and 4% dimethyl sulfoxide (DMSO) as a negative control. The samples were incubated at 35°C for 24 h, and the ZOI diameter was measured in millimeters [11, 13 and 14].

The minimum inhibitory concentration (MIC) and the minimum bactericidal concentration (MBC) were determined by the microdilution method. Initially, the main stocks of AgNPs and Fe_3O_4 NPs were prepared; 1 mg of NPs was added to 10 ml of normal saline and sonicated at 40 kHz for half an hour (equivalent to 100 µg ml^{-1}). Subsequently, the serial dilutions were created in different tubes as 2.5, 5, 10, 20, 40 and 80 µg ml^{-1}, respectively. After adding 20 µl of the pre-prepared bacterial suspension and 1 ml of the Tryptic Soy Broth (TSB) medium to each tube, the incubation was performed at 35°C for 24 h. The positive control was a medium without AgNPs or Fe_3O_4 NPs and with bacteria, as well as the negative control was a medium with AgNPs or Fe_3O_4 NPs and without bacteria. The lowest concentration of the nanoparticle suspension without turbidity was considered the MIC value. The MIC dilutions of 10 µl or more were cultured onto the TSB medium and incubated at 35°C for 24 h. The lowest concentration capable of decreasing the bacterial growth by 99.99% exhibited the MBC value [11, 13, 15].

The collected data were analyzed by the SPSS Version 20 software. One-way analysis of variance (ANOVA) test was conducted to assess the fabrication of AgNPs and Fe_3O_4 NPs and their antimicrobial activity. The mean comparison was performed by Duncan's test at a significance level of 5%. All data were reported as the mean ± standard deviation (SD), and analyses were conducted in triplicate.

RESULTS AND DISCUSSION

The produced NPs were confirmed by two methods of spectrophotometry and SEM imaging. The maximum OD values for AgNPs and Fe_3O_4 NPs were determined at 420 and 215 nm, respectively, confirming the production of NPs. AgNPs and Fe_3O_4 NPs were produced using the *Erodium cicutarium* plant extract, and the highest wavelengths were read at 420 and 230 nm, respectively, being consistent with our study results.

Fe_3O_4 NPs were fabricated with uniform dispersion in *F. solani*, and achieved the greatest OD values at 250-350 nm [4]. According to our study, it was the highest wavelength for AgNPs at 430 nm [11]. In addition, a wavelength of 420 nm was observed for AgNPs produced in marine bacteria [16]. The highest OD value read for Fe_3O_4 NPs was 220 nm in one study conducted by Ghani et al., being in line with the current study results [17].

According to the SEM images, the produced AgNPs exhibited a uniform spherical morphology; however, other shapes were also observed sporadically. The mean size was 27.5-58.3 nm for AgNPs, with 80% in this range (Figure 1a). The produced Fe_3O_4 NPs were in spherical and cubic shapes, as well as in other irregular shapes sporadically. Some produced particles were accumulated in the microscopic view; however, there was no direct contact between the particles due to their relative stability. The produced nanoparticle stability was due to the production of secondary metabolites originating from the bacterial protein coating the nanoparticles. The mean size was 55.3-84.2 nm for Fe_3O_4 NPs (Figure 1b). Some researchers provided reports suggesting similar results, and the particle size was less than 100 nm, and the produced NPs had

different ranges depending on the used microbial strains. The particle shapes in these studies were mostly spherical to cubic forms [4, 16-17].

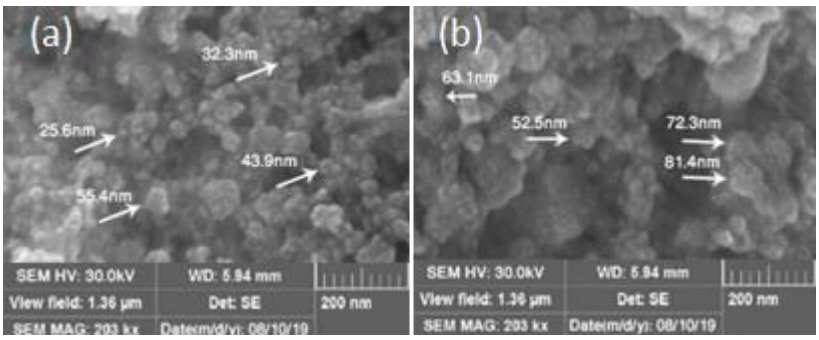

Figure1. SEM images of (a) silver NPs, and (b) iron oxide NPs synthesized by *Fusarium solani*

Figure 2 presents the X-ray diffraction (XRD) pattern of the prepared samples. Analysis of the XRD results of AgNPs synthesized by *Fusarium solani* confirmed the crystalline nature of AgNPs and demonstrated some characteristic peaks at 28.53°, 32.03°, 40.83°, and 45.58° two theta (2θ) values corresponding to (210), (113), (141), and (124) plans of silver NPs, respectively [16]. As Figure 2b shows, the four main peaks observed for the orthorhombic phase of Fe_3O_4 NPs synthesized by *Fusarium solani* at 31.78°, 38.33°, 45.63°, and 56.63° 2θ values corresponding to (220), (311), (400), and (511) plans of Fe_3O_4 NPs, respectively [12]. Thus, iron oxide and silver nanoparticles with well-defined dimensions could be synthesized by reduction of metal ions due to the fungal extract of *Fusarium solani*.

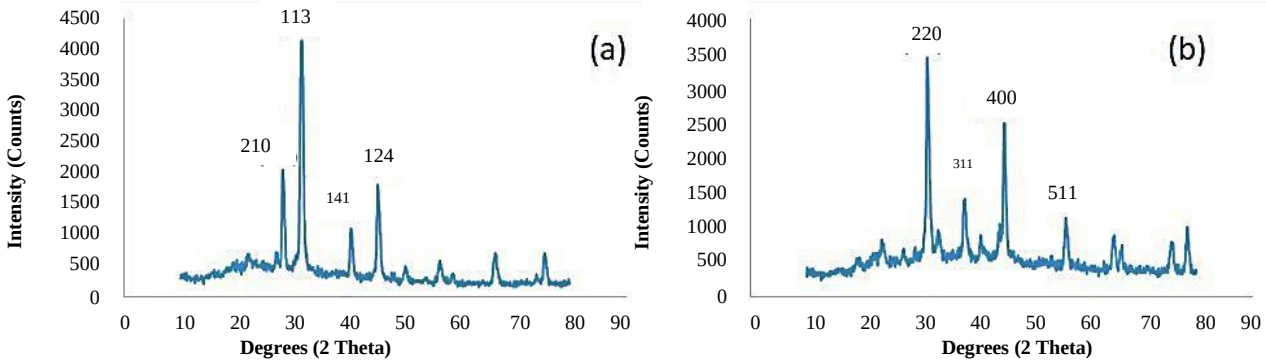

Figure 2. XRD pattern of (a) silver NPs, and (b) iron oxide NPs synthesized by *Fusarium solani*.

Figure 3a (dashed line) depicts the Fourier-transform infrared (FTIR) spectra of synthesized silver NPs. FTIR measurement was performed to identify possible biomolecules of the *Fusarium solani* fungal extract responsible for the formation and stabilization of silver NPs. It was used to identify the characteristic functional groups involved in the formation of AgNPs. The FTIR spectral peaks appeared near 3462.79 cm^{-1} assigned to the hydroxyl (–O-H) and amine (–N-H) stretching due to the presence of amines and water [13]. Peaks at 2925.88 cm^{-1} are due to vibrations of the C-H stretching of alkanes associated with flavonoid molecules. The absorption peak at 1637.46 cm^{-1} can be assigned to the C–O-H carboxylic group stretching in carboxylate. A peak at 1082.47 cm^{-1} is due to vibrations of the C-O stretching of alcoholic groups. The peak near 1000 cm^{-1} was assigned to $C=CH_2$, and the peaks at 619.44 cm^{-1} and 525.99 cm^{-1} were attributed to the CH out of plane bending vibrations, which were substituted ethylene systems –CH=CH [15]. Therefore, the bioreduction of silver (I) into Ag NPs may be attributed to the presence of phenols, flavonoids, amino groups, alkanes, and alkenes present in *Fusarium solani*.

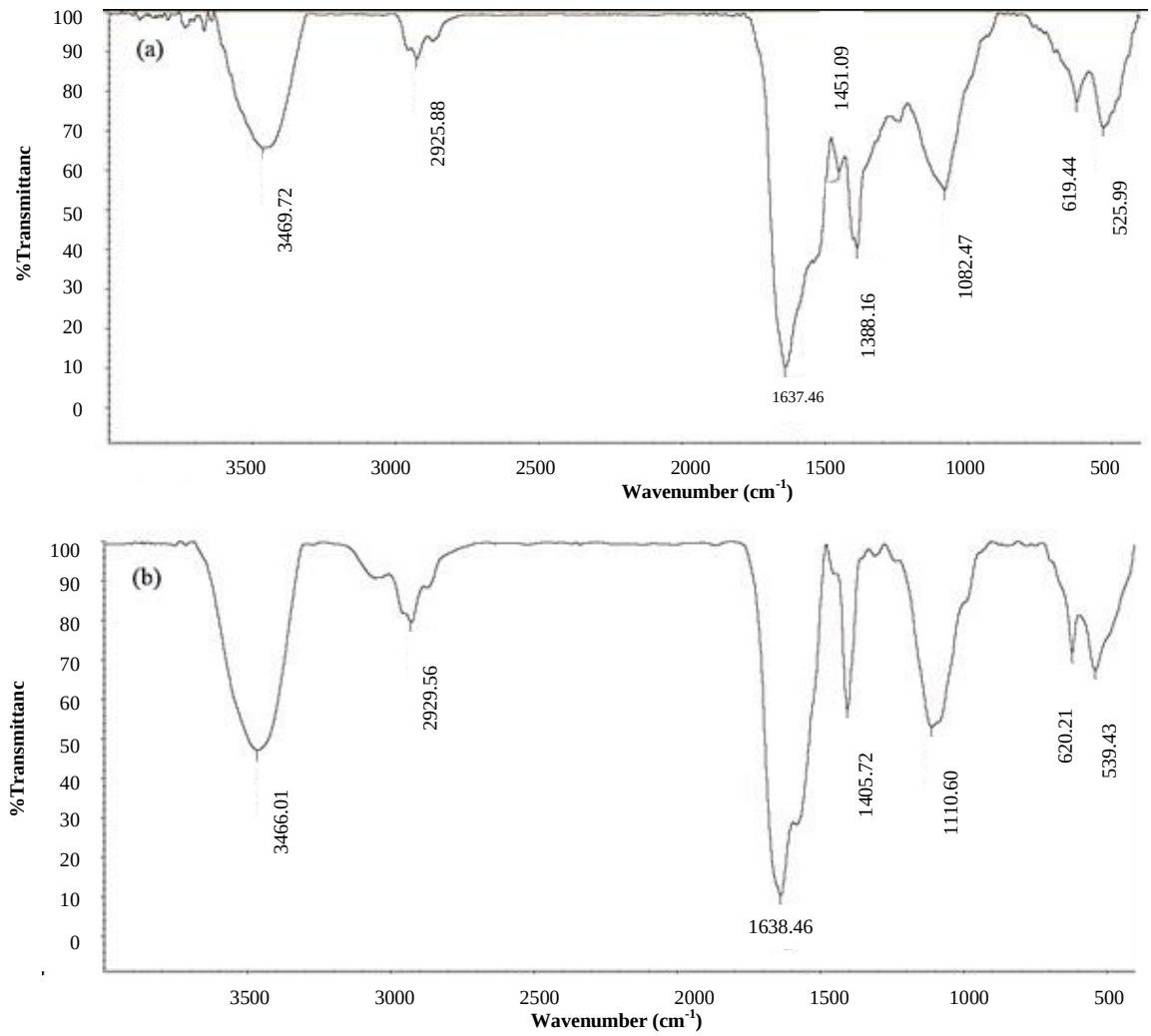

Figure 3. FTIR spectra of (a) silver NPs, and (b) iron oxide NPs synthesized by *Fusarium solani*.

Figure 3b presents the FTIR spectra of synthesized iron oxide NPs using *Fusarium solani*. Peaks at 3399.01 cm^{-1} are assigned to the O-H stretching of alcohols and phenols. A peak near 2929.56 cm^{-1} indicates the presence of CH stretching groups. The absorption peak at 1638.46 cm^{-1} can be assigned to the C–O-H carboxylic group stretching in carboxylate. In addition, the peak near 1405.72 cm^{-1} may be assigned to the presence of carboxylate ions (COO-), being responsible for the formation of iron oxide NPs. The formation of Fe_3O_4 NPs is characterized by the absorption band near 539.43 cm^{-1} corresponding to the Fe–O bond [12].

Evaluation of antibacterial activity

Measurement of the ZOI diameter

Table 1 shows the results of the analysis of antimicrobial effects by the agar well diffusion method for AgNPs produced by *F. solani.* As Table 1 shows, there is a significant difference in antimicrobial effects between the selected antibiotics and AgNP ($P < 0.05$).

Among the studied bacteria, *S. aureus* and *P. aeruginosa* were the most sensitive and resistant bacteria, respectively. Overall, gram-positive bacteria were more sensitive to antimicrobials than gram-negative bacteria were; this can be attributed to the existence of lipopolysaccharide and lipid layers in the structure of the gram-negative bacterial cell wall; this is not always true, and gram-positive bacteria can also be more resistant in some cases.

Table 1. Inhibitory effects of silver nanoparticles synthesized with *Fusarium solani* cell mass on the indicator bacteria using agar well diffusion method

Bacteria	50 µl	100 µl	Ampicillin	Gentamicin	Silver nitrate
Staphylococcus aureus	17±0.1cA	23±0.1bA	30±0.5a	-	10±0.2dA
Bacillus cereus	10±0.2cBC	13±0.4bB	26±0.2a	-	10±0.1dA
Pseudomonas aeruginosa	7±0.2cD	10±0.3bBC	-	18.5±0.3a	7±0.2cAB
Escherichia coli	11±0.3cBC	13±0.2bCD	-	24±0.2a	9±0.1dA

Different capital and lowercase letters in each row and column show a significant difference in the data (P<0.05)

Table 2 shows the antimicrobial test results exploiting the agar well diffusion method for Fe_3O_4 NPs produced by *F. solani*. There was a significant difference in the antimicrobial effects between the selected antibiotics and Fe_3O_4 NPs (P<0.05). Among the tested bacteria, *S. aureus* and *P. aeruginosa* were the most sensitive and resistant bacteria, respectively. Based on the findings, the antimicrobial effects of AgNPs were stronger than those of Fe_3O_4 NPs. The silver nitrate is currently employed as a common antimicrobial agent, since it has bacteriostatic and bactericidal activity on most pathogenic and indicator bacteria. The antimicrobial potential of AgNPs fabricated from silver is increased owing to its very high reactivity and higher contact surface. Normally, iron oxide has no antimicrobial effect, but in the form of nanoparticles, it can achieve antimicrobial properties and inhibit the further growth of indicator bacteria. Hence, higher activity of AgNPs in bacterial growth inhibition is due to the intrinsic antimicrobial capacity of silver metal, which doubles after converting into NPs [18-21].

Table 2. Inhibitory effects of iron oxide nanoparticles synthesized by *Fusarium solani* cell mass on the indicator bacteria using agar well diffusion method

Bacteria	50 µl	100 µl	Ampicillin	Gentamicin	Iron oxide
Staphylococcus aureus	12±0.3cB	15±0.2bB	30±0.5a	-	0
Bacillus cereus	10±0.3cB	12.5±0.2bCD	26±0.2a	-	0
Pseudomonas aeruginosa	7±0.1cD	10±0.4bE	-	18.5±0.3a	0
Escherichia coli	9±0.3cBC	12.5±0.2bCD	-	24±0.2a	0

Different capital and lowercase letters in each row and column show a significant difference in the data (P<0.05)

Determination of MIC and MBC values

Tables 3 and 4 show the MIC and MBC values obtained for AgNPs and Fe_3O_4 NPs against indicator bacteria. The results indicated the highest and lowest MIC values of AgNPs for *S. aureus* and *P. aeruginosa* as 10 and 40 µg ml^{-1}, respectively. Furthermore, the MBC values of AgNPs for these two bacteria were 20 and 80 µg ml^{-1}, respectively; this, similar to the results of the agar well diffusion method, demonstrated the high resistance of *P. aeruginosa* and the sensitivity of *S. aureus* to the concentrations of AgNPs used. The results revealed that the bacteriostatic and bactericidal effects of Fe_3O_4 NPs on indicator bacteria were weaker than those of AgNPs, so that the MIC of 20 µg ml^{-1} was detected for *B. cereus* and *S. aureus* as well as 40 µg ml^{-1} for *P. aeruginosa* and *E. coli*, with the MBC values of 80 and 40 µg ml^{-1}, respectively.

Table 3. Results of the minimum inhibitory concentration (MIC) and the minimum bactericidal concentration (MBC) of silver nanoparticles produced by *Fusarium solani* against indicator bacteria using the microdilution method

Bacteria	MIC (µg ml^{-1})	MBC (µg ml^{-1})
Staphylococcus aureus	10	20
Bacillus cereus	20	40
Pseudomonas aeruginosa	40	80
Escherichia coli	20	40

Table 4. Results of the minimum inhibitory concentration (MIC) and the minimum bactericidal concentration (MBC) of iron oxide nanoparticles produced by *Fusarium solani* against indicator bacteria using the microdilution method

Bacteria	MIC (µg ml^{-1})	MBC (µg ml^{-1})
Staphylococcus aureus	20	40
Bacillus cereus	20	40
Pseudomonas aeruginosa	40	80
Escherichia coli	40	80

It was reported that the MIC values of Fe_3O_4 NPs and AgNPs produced in the *Cicutarium erodium* plant extract against *S. aureus* and *E. coli* were 399.53 and 397.38 µg ml^{-1}, respectively. They found that the antibacterial activity of Fe_3O_4 NPs was slightly greater than that of AgNPs. The MIC value of NPs produced in the plant was much higher than that of our study [12]. AgNPs synthesized from Fusarium have antimicrobial potential and affect the growth of *Candida albicans*, *E. coli*, *Candida krusei*, *S. aureus* and *Aspergillus flavus* [10]. The effects of AgNPs produced in the present study were stronger than those of the above study, so that the diameter of ZOI was more evident in *S. aureus* and *E. coli*. Begam (2016) found that 30 µl of AgNPs had more antibacterial effects than 15 µl of AgNPs, with *Salmonella typhimurium* being the most sensitive bacterium (with the ZOI diameter of 15 mm) and *Klebsiella pneumoniae* being the most resistant bacterium [16].

Higher antimicrobial effects of NP iron nitrate were observed; however, no antimicrobial activity was noticed for iron nitrate alone; further, *P. aeruginosa* and *E. coli* had more sensitivity than bacterial strains, according to the current study [17]. The MIC and MBC test results were the same as the findings of the ZOI test, with the values of 0.015 and 0.008 mg L^{-1} against *P. aeruginosa* and *E. coli*, respectively, but 0.031 mg L^{-1} against *B. cereus* and *S. aureus*, being inconsistent with our results.

ZOI test results were reported for the Fe_3O_4 NPs fabricated by Alternaria similar to our study, so that *P. aeruginosa* was the most resistant bacterium, and *B. cereus* was the most sensitive bacterium [11]. It was reported that the antibacterial and antitumor properties of AgNPs synthesized from *F. oxysporum*, and found that 80 µl of AgNPs had inhibitory effects against *E. coli* and *S. aureus* [9]; however, the results were much weaker than those of the present study (at both 50 and 100 µl concentrations). In general, smaller AgNPs exhibited greater inhibitory effects due to higher contact surface, and gram-positive bacteria were more sensitive than gram-negative bacteria [22-30]. Recently, it has been reported that AgNPs synthesized from Aspergillus have inhibitory effects on methicillin-resistant *Staphylococcus aureus* [25]. Due to the high contact surface, the antibacterial effects of AgNPs were higher than those of pure silver ions [31-40]. It has been found that the combination of AgNPs and some antibiotics significantly increases antibacterial effects [25].

CONCLUSIONS

According to the present study results, *Fusarium solani* could prepare both iron oxide and silver nanoparticles, with the maximum wavelengths ranging from 215 to 420 nm, respectively. The scanning electron microscope images displayed a smaller size and a spherical shape for silver nanoparticles, but exhibited larger size and spherical to cubic shapes for iron oxide nanoparticles. Overall, silver nanoparticles showed better antibacterial activity than iron oxide nanoparticles did. *Staphylococcus aureus* and *Pseudomonas aeruginosa* were the most sensitive and resistant bacteria, respectively. In this work, *Escherichia coli* and *Bacillus cereus* were intermediate. The antimicrobial properties of these nanoparticles suggest that iron oxide and silver NPs can act as bio-alternatives and eco-friendly agents to reduce microbial contaminants, especially indicator bacteria in water to promote the health and food safety of different societies.

ADDITIONAL INFORMATION AND DECLARATIONS

Ethics approval and consent to participate

All authors accept the ethics of publishing and are not barred from participating in the article as authors.

Consent for publication

All authors will be satisfied with the publication of this article.

Availability of data and materials

This article has been adapted from a PhD dissertation written by Ms. Masoumeh Sasani. Therefore, its data can be received through them if necessary.

Competing interests

The authors declare no competing interests.

Funding

This research was funded by the student herself (Ms. Sasani) and had no financial support.

Authors' contributions

In this study, Ms. Masoumeh Sasani as a PhD student, and Dr. Ebrahim Fataei and Dr. Reza Safari as the first and second supervisors, respectively, and Dr. Fatemeh Nasehi and Dr. Marzieh Mosayebi as advisors contributed to this PhD dissertation, respectively.

ACKNOWLEDGEMENTS

This article was extracted from a PhD degree thesis. We would like to thank Islamic Azad University, Ardabil Branch, for providing the opportunity to pursue a PhD degree and conducting this research in the Department of Environmental Science and Engineering.

REFERENCES

1. Singh P., Singh H., Kim Y.J., Mathiyalagan R., Wang C., Yang D.C., 2016. Extracellular synthesis of silver and goldnanoparticles by Sporosarcina koreensis DC4 andtheir biological applications. Enzyme Microb Technol. 86, 75-83.

2. Kaviya S., Santhanalakshmi J., Viswanathan B., Muthumary J., Srinivasan K., 2011. Biosynthesis of silver nanoparticlesusing citrus sinensis peel extract and itsantibacterial activity. Spectrochim Acta Mol Biomol Spe. 79, 594-98.

3. Kim S.H., Lee H.S., Ryu D.S., Choi S.J., Lee D.S., 2011. Antibacterial activity of silver-nanoparticles against*Staphylococcus aureus* and *Escherichia coli*. Korean J Microbiol Biotechnol. 39(1), 77-85.

4. Sundaram P.A., Augustine R., Kannan M., 2012. Extracellular Biosynthesis of Iron Oxide Nanoparticles by *Fusarium solani* Strains Isolated from Rhizosphere Soil. Biotechnology and Bioprocess Engineering. 17, 835-840.

5. Jianrong C., Yuqing M., Nongyue H., Xiaohua W., Sijiao L., 2004. Nanotechnology andbiosensors. Biotech Adv. 22, 505-18.

6. Nanda A., Saravanan M., 2009. Biosynthesis of silver nanoparticles from Staphylococcus aureus and its antimicrobialactivity against MRSA and MRSE. Nanomedicine. 5(4), 452-456.

7. Ahmad A., Mukherjee P., Senapati S., Mandal D., Islam Khan M., Kumar R., 2003. Extracellular biosynthesis of silvernanoparticles using the fungus *Fusarium oxysporum*. Colloids Surf B Biointerfaces. 28(4), 313-318.

8. Pourali P., Baseri Salehi M., Afsharnezhad S., Behravan J., 2013. Biological production and assessment of the antibacterial activity of gold nanoparticles. Journal of Microbial World. 6(3), 198-211.

9. Husseiny S.M., Salah T.A., Anter H.A., 2015. Biosynthesis of size controlled silver nanoparticles by Fusarium oxysporum, their antibacterial and antitumor activities. Beni-Suef University Journal of Basic and Applied Sciences. 4, 225-231.

10. Tabassum Khan N.T., Jameel M., Jameel J., 2017. Silver Nanoparticles biosynthesis by Fusarium oxysporum and determination of its antimicrobial potency. J Nanomedine Biotherapeutic Discov. 7(1), 1-3.

11. Mahmoud W.M., Abdelmoneim T.S., Elazzazy A.M., 2015. The impact of silver nanoparticles produced by Bacilluspumilus as antimicrobial and nematicide. Frontiers in Microbiology. 7, 1-9.

12. Maghsoudy N., Aberoomand Azar P., Saber Tehrani M., 2019. Biosynthesis of Ag and Fe nanoparticles using *Erodium cicutarium*; study, optimization, and modeling of the antibacterial properties using response surface methodology. Journal of Nanostructure in Chemistry. 9, 203–216.

13. Garmasheva I., Kovalenko N., Voychuk S., 2016. *Lactobacillus* species mediated synthesis of silver nanoparticles and their antibacterial activity against opportunistic pathogens *in vitro*. BioImpacts. 6(4), 219-223.

14. Omrani M., Fataei E., 2018. Synthesizing Colloidal Zinc Oxide Nanoparticles for Effective Disinfection; Impact on the Inhibitory Growth of Pseudomonas aeruginosa on the Surface of an Infectious Unit, Pol. J Environ Stud. 27(4), 1639-1645.

15. Gudikandula K., Charya Maringanti S., 2016. Synthesis of silver nanoparticles by chemical and biological methods and their antimicrobial properties, Journal of Experimental Nanoscience. 11(9), 714-721.

16. Begam J.N., 2016. Biosynthesis and characterization of silver nanoparticles (AgNPs) using marine bacteria against certain human pathogens. J. Nasrin /International Journal of Advances in Scientific Research. 2(7), 152-156.

17. Ghani S., Rafiee B., Sadeghi D., Ahsani M., 2017. Biosynthesis of Iron Nano-Particles by Bacillus Megaterium and Its Anti-Bacterial Properties. J Babol Univ Med Sci. 19(7), 13-19.

18. Abdul Fatima R., Subhi H.T., Taher N.A., 2019. Activity of Iron oxide nanoparticles on bacterial biofilm formation. Journal of pharmaceutical Sciences and Research. 11(3), 1126-1130.

19. Matei A., Matei S., Matei G.M., 2020. Biosynthesis of silver nanoparticles mediated by culture filtrate of lactic acid bacteria, characterization and antifungal activity. Research Article Pharmaceutical Biotechnology. 4(2), 97-103.

20. John M.S., Nagoth J.A., Ramasamy A.M., 2020. Synthesis of Bioactive Silver Nanoparticles by a Pseudomonas Strain Associated with the Antarctic Psychrophilic Protozoon Euplotes focardii. Marine Drugs. 18(38), 1-13.

21. Çelik S., Oltulu M., Jafarian Barough M., Mohammadi Aloucheh R., 2021. Application of Nanomaterials for Increase of Compressive Strength on Granular Soils to Attain Minimal Damage to the Environment, Anthropogenic Pollution. 5(1), 105-111.

22. Vanaja M., Annadurai G., 2013. Coleus aromaticus leaf extract mediated synthesis of silver nanoparticles and its bactericidal activity. Appl Nanosci. 3, 217–223.

23. Das J., Das M.P., Velusamy P., 2013. Sesbania grandiflora leaf extract mediated green synthesis of antibacterial silver nanoparticles against selected human pathogens. Spectrochim Acta Part A Mol Biomol Spectrosc. 104, 265-270.

24. Singh D., Rathod V., Ninganagouda S., Hiremath J., Singh A.K., Mathew J., 2014. Optimization and characterization of silver nanoparticle by endophytic fungi Penicillium sp. isolated from Curcuma longa (turmeric) and application studies against MDR *Escherichia coli* and *Staphylococcus aureus*. Hindawi Publish Corpor Bioinorg Chem Appl. 2014, 1-8.

25. Magdi H.M., Mourad M.H.E., Abd El-Aziz M.M., 2014. Biosynthesis of silver nanoparticles using fungi and biological evaluation of mycosynthesized silver nanoparticles. Egypt J Exp Biol. 10(1), 1–12.

26. Cho K.H., Park J.E., Osaka T., Park S.G., 2005. The study of antimicrobial activity and preservative effects of nanosilver ingredient. Elecrtochemica Acta. 51(5), 956-960.

27. Panyala N.R., Pena-Mendez E.M., Havel J., 2008. Silver or silver nanoparticles: a hazardous threat to the environment and human health. J Appl Biomed. 6(3), 117–129.

28. Safarkar R., Ebrahimzadeh Rajaei G., Khalili-arjaghi S., 2020. The study of antibacterial properties of iron oxide nanoparticles synthesized using the extract of lichen Ramalina sinensis. Asian Journal of Nanoscience and Materials. 3, 157-166.

29. Khalili Arjaghi S., Kashfi Alasl M., Sajjadi N., Fataei E., Ebrahimzadeh Rajaei G., 2021. Green Synthesis of Iron Oxide Nanoparticles by RS Lichen Extract and its Application in Removing Heavy Metals of Lead and Cadmium, Biological Trace Element Research. 199(2), 763-768.

30. Khalili Arjaghi S., Ebrahimzadeh Rajaei G., Sajjadi N., Kashfi Alasl M., Fataei E., 2020. Removal of Mercury and Arsenic Metal Pollutants from Water Using Iron Oxide Nanoparticles Synthesized from Lichen

Sinensis Ramalina Extract. Journal of Health. 11(3), 397-408.

31. Ebrahimzadeh Rajaei G., Khalili Arjaghi S., Fataei E., Sajjadi N., Kashfi Alasl M., 2020. Fabrication and characterization of polymer-based nanocomposite membrane modified by magnetite nanoparticles for Cd and Pb removal from aqueous solutions, Comptes Rendus. Chimie. 23(9-10), 563-574.

32. Rajaei G.E., Aghaie H., Zare K., Aghaie M., 2013. Adsorption of Cu (II) and Zn (II) ions from aqueous solutions onto fine powder of Typha latifolia L. root: kinetics and isotherm studies, Research on Chemical Intermediates. 39(8), 3579-3594.

33. Ebrahimzadeh Rajaei G., Aghaie H., Zare K., Aghaie M., 2021. Adsorption of Ni (II) and Cd (II) ions from aqueous solutions by modified surface of Typha latifolia L. root, as an economical adsorbent. Journal of Physical & Theoretical Chemistry. 9, 137-147.

34. Rezaei-Aghdam E., Shamel A., Khodadadi-Moghaddam M., Rajaei G.E., Mohajeri S., 2021. Synthesis of TiO_2 and ZnO Nanoparticles and CTAB-Stabilized Fe_3O_4 nanocomposite: kinetics and thermodynamics of adsorption. Research on Chemical Intermediates. 47, 1759-1774.

35. Nokandeh M., Khoshmanesh B., 2019. Removal of Acid Yellow-36 Dye from textile industries waste water using photocatalytic process (UV/TiO_2), Anthropogenic Pollution Journal. 3(2), 10-17.

36. Gooran Ourimi H., Nezhadnaderi M., 2020. Comparison of the application of Heavy metals adsorption methods from aqueous solutions for development of sustainable environment, Anthropogenic Pollution Journal. 4(2), 15-27.

37. Sadr S., Ershad Langroudi A., Nejaei A., Rabiee A., Mansouri N., 2021. Arsenic and Lead Removal from Water by Nano-photocatalytic Systems (A Review). Anthropogenic Pollution Journal. 5(1), 72-80.

38. Rashtbari Y., Américo-Pinheiro J.H.P., Bahrami S., Fazlzadeh M., Arfaeinia H., Poureshgh Y., Efficiency of zeolite coated with zero-valent iron nanoparticles for removal of humic acid from aqueous solutions. Water, Air, & Soil Pollution. 231(10). (In Press).

39. Rashtbari Y., Afshin S., Hamzezadeh A., Abazari M., Poureshgh Y., Fazlzadeh M., 2020. Application of powdered activated carbon coated with zinc oxide nanoparticles prepared using a green synthesis in removal of Reactive Blue 19 and Reactive Black-5: adsorption isotherm and kinetic models, Desalination & Water Treatment. 179, 354-367.

40. Ali I., Afshinb S., Poureshgh Y., Azari A., Rashtbari Y., Feizizadeh A., Hamzezadeh A., Fazlzadeh M., 2020. Green preparation of activated carbon from pomegranate peel coated with zero-valent iron nanoparticles (nZVI) and isotherm and kinetic studies of amoxicillin removal in water. Environmental Science and Pollution Research. 27, 36732–36743.